

TEST OF A 1.8 TESLA, 400 HZ DIPOLE FOR A MUON SYNCHROTRON*

D. J. Summers[†], L. M. Cremaldi, T. L. Hart, L. P. Perera, M. Reep,
 University of Mississippi- Oxford, University, MS 38677, USA
 H. Witte, Brookhaven National Lab, Upton, NY 11973, USA
 S. Hansen, M. L. Lopes, Fermilab, Batavia, IL 60510, USA
 J. Reidy, Jr., Oxford High School, Oxford, MS 38655, USA

Abstract

A 1.8 T dipole magnet using thin grain oriented silicon steel laminations has been constructed as a prototype for a muon synchrotron ramping at 400 Hz. Following the practice in large 3 phase transformers and our own Opera-2d simulations, joints are mitred to take advantage of the magnetic properties of the steel which are much better in the direction in which the steel was rolled. Measurements with a Hysteresigraph 5500 and Epstein frame show a high magnetic permeability which minimizes stored energy in the yoke allowing the magnet to ramp quickly with modest voltage. Coercivity is low which minimizes hysteresis losses. A power supply with a fast Insulated Gate Bipolar Transistor (IGBT) switch and a capacitor was constructed. Coils are wound with 12 gauge copper wire. Thin wire and laminations minimize eddy current losses. The magnetic field was measured with a peak sensing Hall probe.

INTRODUCTION

A muon collider [1] is perhaps unparalleled for exploring the energy frontier, if an economical design for muon cooling and acceleration can be finalized. Historically synchrotrons have provided low cost acceleration. Here we present results on a dipole magnet prototype for a relatively fast 400 Hz synchrotron [2] for muons, which live for 2.2 μ s. Low emittance muon bunches allow small apertures and permit magnets to ramp with a few thousand volts, if the $B^2/2\mu$ energy stored in the magnetic yoke is kept low.

DIPOLE CONSTRUCTION AND RESULTS

To minimize energy stored in the magnetic yoke, grain oriented silicon steel was chosen due to its high permeability as noted in Table 1. Thin 0.011" AK Steel TRAN-COR H-1 laminations and 12 gauge copper wire minimize eddy current losses which go as the square of thickness [3]. The copper wire will eventually be cooled with water flowing in stainless steel tubes [4]. The very low coercivity of grain oriented silicon steel as noted in Table 2 minimizes hysteresis losses [5]. The power supply is an LC circuit with a 52 μ F polypropylene capacitor and a fast IGBT Powerex CM600HX-24A switch. The magnet gap is 1.5 x 36 x 46 mm and $f = 1/2\pi\sqrt{LC}$. The energy stored in the gap is:

$$W = \int \frac{B^2}{2\mu_0} dh dw d\ell = \frac{LI^2}{2} = \frac{CV^2}{2} = 3.2 \text{ J}$$

* Work supported by NSF 757938 and DOE DE-FG05-91ER40622

[†] summers@phy.olemiss.edu

An ideal dipole with $N = 40$ turns of copper wire and a current of $I = Bh/\mu_0 N = 54 \text{ A}$ would require a voltage of $V = 2\pi BfNw\ell = 315 \text{ V}$ to generate 1.8 T at 400 Hz.

Table 1: Relative permeability (μ/μ_0) for 3% grain oriented silicon steel [6] as a function of angle to the rolling direction. Dipole magnetic flux needs to be parallel to the rolling direction. The minimum at 1.3 T and 55° comes from the long diagonal (111) of the steel crystal.

	0.1T	0.7T	1.3T	1.5T	1.7T	1.8T	1.9T	2.0T
0°	29000	46000	49000	48000	30000	14000	6000	180
10°	8000	14000	14000	10000	3000			
20°	3500	9800	9000	2100				
55°	700	3800	540					
90°	660	3300	2300	320	120	80	60	50

Table 2: Soft magnetic steel properties.

Steel	ρ $\mu\Omega\cdot\text{cm}$	H_c Oersteds	μ/μ_0 @B(T)
Oriented 3% silicon [6]	46	0.09	14000@1.8
Ultra low carbon [7]	10	0.5	1900@1.5
3% silicon	46	0.7	1600@1.3
JFE 6.5% silicon	82	0.2	1500@1.3
Hiperco 50A (49Fe:49Co)	42	0.3	2100@2.1

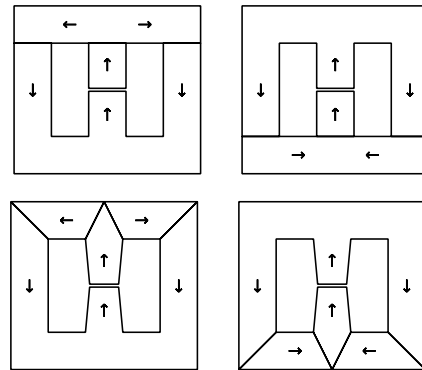


Figure 1: Dipole laminations with butt and mitred joints.

Our first dipole prototype was made with butt joints as shown on the top of Fig. 1. The mitred joints in the second prototype as shown on the bottom of Fig. 1 work better.

To further explore mitred joints, an Opera-2d simulation as shown in Fig. 2 was run. Opera-2d only allows magnetic properties in the x and y directions to be entered. It then uses a $\mu_\theta = [(\cos\theta/\mu_{0^\circ})^2 + (\sin\theta/\mu_{90^\circ})^2]^{-0.5}$ ellipti-

cal approximation. This is problematic for grain oriented silicon steel which has a minimum permeability at μ_{55° .

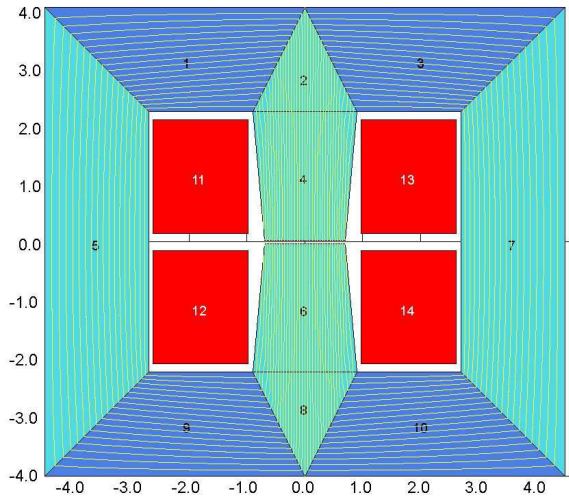


Figure 2: Opera-2d simulation of a mitred joint dipole. It worked, but there were some problems with convergence.

In two dimensions [8]:

$$\frac{\partial^2 A}{\partial x^2} + \frac{\partial^2 A}{\partial y^2} - \frac{1}{\mu} \frac{\partial \mu}{\partial x} \frac{\partial A}{\partial x} - \frac{1}{\mu} \frac{\partial \mu}{\partial y} \frac{\partial A}{\partial y} = -\mu J_z$$

where $\nabla \cdot A = 0$ and $A = A_z$. Thus $B_x = -\frac{\partial A}{\partial y}$, $B_y = -\frac{\partial A}{\partial x}$, and $\theta = \text{atan}(B_y/B_x)$ are available for finite element iterations. The following subroutine generates a BH curve at any angle using linear interpolation of a table with 5 angles.

```

SUBROUTINE BH(NP, ANG, FANG, PM1, PM2, PM3, PM4, PM5, PM)
IMPLICIT NONE
INTEGER NP, J
REAL FANG(5), PM(10), ANG, DANG
REAL PM1(10), PM2(10), PM3(10), PM4(10), PM5(10)
C
IF (ANG.GE.FANG(1) .AND. ANG.LT.FANG(2)) THEN
DO 10 J=1, NP
DANG = (ANG - FANG(1))/(FANG(2) - FANG(1))
10 PM(J) = PM1(J) + DANG*(PM2(J) - PM1(J))
ELSE IF (ANG.GE.FANG(2) .AND. ANG.LT.FANG(3)) THEN
DO 20 J=1, NP
DANG = (ANG - FANG(2))/(FANG(3) - FANG(2))
20 PM(J) = PM2(J) + DANG*(PM3(J) - PM2(J))
ELSE IF (ANG.GE.FANG(3) .AND. ANG.LT.FANG(4)) THEN
DO 30 J=1, NP
DANG = (ANG - FANG(3))/(FANG(4) - FANG(3))
30 PERM(J) = PM3(J) + DANG*(PM4(J) - PM3(J))
ELSE IF (ANG.GE.FANG(4) .AND. ANG.LE.FANG(5)) THEN
DO 40 J=1, NP
DANG = (ANG - FANG(4))/(FANG(5) - FANG(4))
40 PM(J) = PM4(J) + DANG*(PM5(J) - PM4(J))
END IF
RETURN
END

```

To check our steel, the hysteresis loop shown in Fig. 3 was measured with an Epstein frame and Hysteresigraph 5500. Fig. 4 shows our magnet with mitred joints and Fig. 5 shows a permanent magnet used to check Hall probes. DC magnetic tests were run on our two magnets as shown in Fig. 6. The mitred joint magnet starts to become nonlinear at 1.7 T. Fig. 7 shows our fast ramping IGBT power supply. Figs. 8 and 9 show results of ringing our mitred joint dipole.

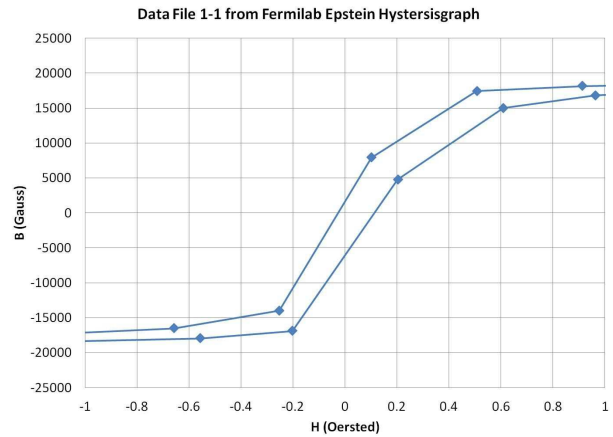


Figure 3: BH(0°) for our steel. $B^2/2\mu$ and H_c are small. $\mu/\mu_0 = 17000$ and 9000 at 1.7 T and 1.81 T, respectively.

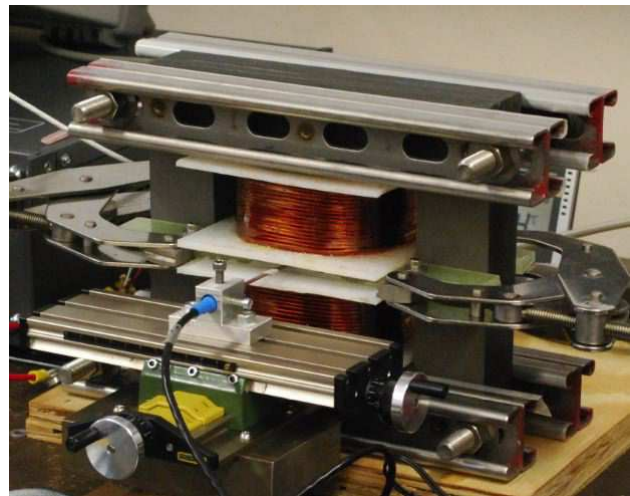


Figure 4: Dipole magnet with mitred laser cut laminations. Laminations were reannealed and recoated after cutting.

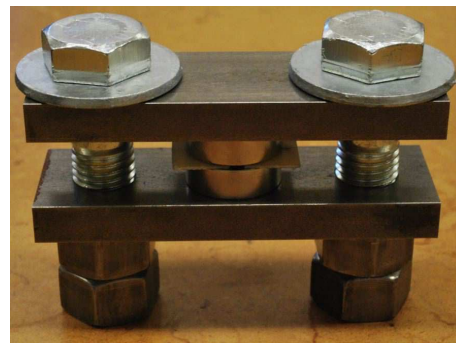


Figure 5: 1.17 T NdFeB magnet with 38 mm diameter pole faces used to check Hall probes.

SUMMARY

A 1.8 T dipole can run at 400 Hz. A magnetic flux circuit with a large yoke path to gap ratio works with high permeability steel. The next step is improving field quality

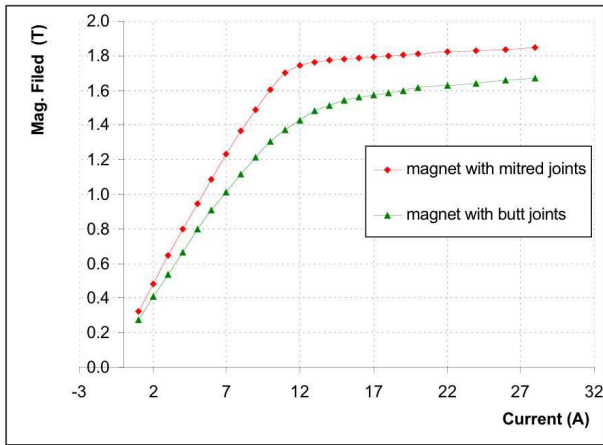


Figure 6: B field vs. current for our butt joint magnet (bottom) and mitred joint magnet (top). B&K Precision 1794 DC linear power supply and F. W. Bell 5180 Hall probe.

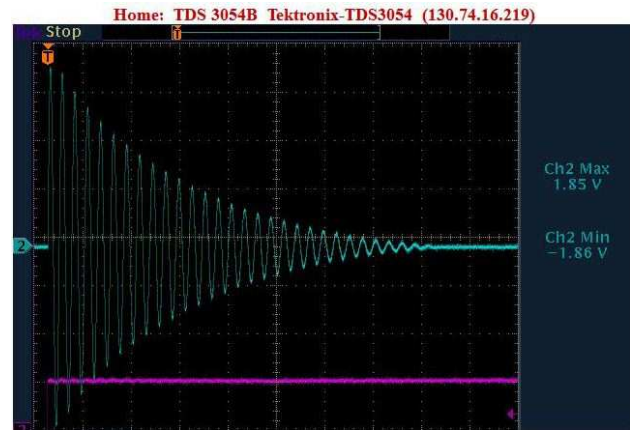


Figure 8: Mitred dipole with 53 turns and 430 V gives 1.81 T at 425 Hz. Energy loss is 10% per half cycle. F. W. Bell 5180 peak sensing Hall probe connected to a Tektronix TDS3054B oscilloscope.

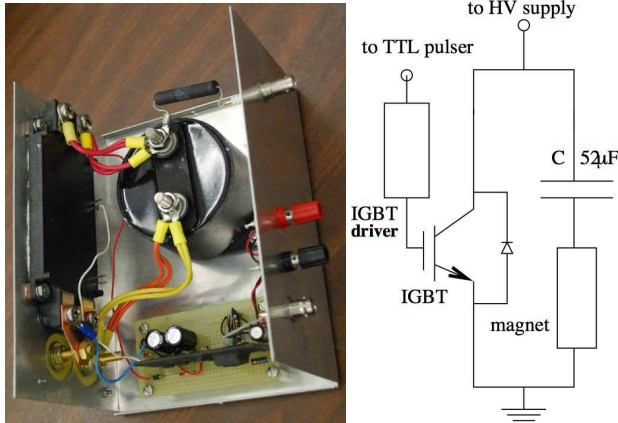


Figure 7: Fast IGBT / 52 μ F capacitor power supply. Powerex CM600HX-24A IGBT and VLA500-01 gate driver.

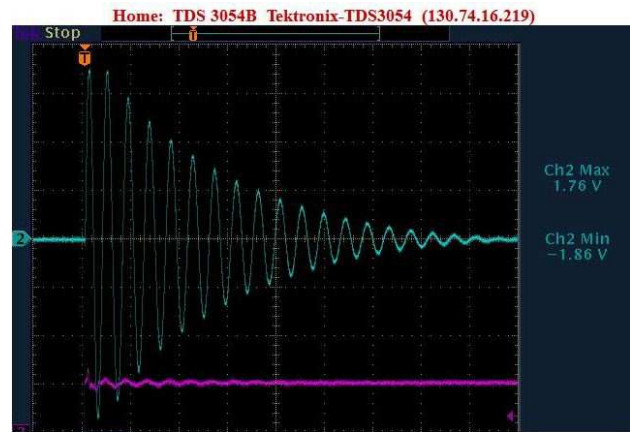


Figure 9: Mitred dipole with 18 turns and 550 V gives 1.81 T at 1410 Hz. Energy loss is 15% per half cycle.

and the accuracy of pole faces, as well as matching calculated and observed losses. Simulation of anisotropic steel has proven challenging. Transverse beam pipe impedance, which is proportional to the inverse cube of beam pipe diameter, will probably dictate a 12 mm dipole gap. Radiation damage of steel needs to be explored [9] and a Rogowski profile needs to be added to magnet ends.

ACKNOWLEDGMENT

Finally, we are most grateful to S. Berg, K. Bourkland, A. Garren, K. Y. Ng, R. Palmer, R. Riley, A. Tollestrup, J. Tompkins, S. Watkins, and J. Zweibohmer for their help.

REFERENCES

[1] D. Neuffer, AIP Conf. Proc. **156** (1987) 201;
 R. Fernow and J. Gallardo, Phys. Rev. **E52** (1995) 1039;
 J. Gallardo *et al.*, Snowmass 1996, BNL-52503;
 C. Ankenbrandt *et al.*, Phys. Rev. ST AB **2** (1999) 081001;
 M. Alsharo'a *et al.*, Phys. Rev. ST AB **6** (2003) 081001;
 R. Palmer *et al.*, Phys. Rev. ST AB **8** (2005) 061003;

R. Palmer *et al.*, arXiv:0711.4275;
 M. Bogomilov *et al.* (MICE Collab.), arXiv:1203.4089;
 R. Palmer *et al.*, Phys. Rev. ST AB **12** (2009) 031002;
 Y. Torun *et al.*, IPAC-2012-THPPC037;
 T. Hart *et al.*, IPAC-2012-MOPPC046;
 G. Lyons *et al.*, IPAC-2012-TUPPR008; arXiv:1112.1105.
 [2] D. J. Summers *et al.*, arXiv:0707.0302; physics/0108001;
 A. A. Garren and J. S. Berg, BNL-96366-2011-IR.
 [3] H. Sasaki, KEK-PREPRINT-91-216.
 [4] S. West *et al.*, EPAC-2008-THPP136;
 N. Tani *et al.*, IEEE Trans. Appl. Supercond. **18** (2008) 314;
 N. Tani *et al.*, IEEE Trans. Appl. Supercond. **14** (2004) 409.
 [5] C. L. Dawes, "Course in Electrical Engineering" (1920) 182.
 [6] G. Shirkoohi and M. Arikat, IEEE Trans. Mag. **30** (1994) 928.
 [7] H. Laeger *et al.*, IEEE Trans. Magnetics **24** (1988) 835;
http://www.cmispecialty.com/31558.CMI-B_Data_Sheet.pdf
 [8] G. Fischer, AIP Conf. Proc. **153** (1987) 1120.
 [9] D. Park *et al.*, IEEE Trans. Magnetics **34** (1998) 2036.